W-Band waveguide filters fabricated by laser micromachining and 3-D printing

Shang, Xiaobang; Penchev, Pavel; Guo, Cheng; Lancaster, Michael J.; Dimov, Stefan; Dong, Yuliang; Favre, Mirko; Billod, Mathieu; De Rijk, Emile

DOI:
10.1109/TMTT.2016.2574839

W-Band Waveguide Filters Fabricated by Laser Micromachining and 3-D Printing

Xiaobang Shang, *Member, IEEE*, Pavel Penchev, Cheng Guo, Michael J. Lancaster, *Senior Member, IEEE*, Stefan Dimov, Yuliang Dong, Mirko Favre, Mathieu Billod, and Emile de Rijk

***Abstract*— This paper presents two W-band waveguide bandpass filters, one fabricated using laser micromachining and the other 3-D printing. Both filters are based on coupled resonators and are designed to have a Chebyshev response. The first filter is for laser micromachining and it is designed to have a compact structure allowing the whole filter to be made from a single metal workpiece. This eliminates the need to split the filter into several layers and therefore yields an enhanced performance in terms of low insertion loss and good durability. The second filter is produced from polymer resin using a stereolithography 3-D printing technique and the whole filter is plated with copper. To facilitate the plating process, the waveguide filter consists of slots on both the broadside and narrow side walls. Such slots also reduce the weight of the filter while still retaining the filter's performance in terms of insertion loss. Both filters are fabricated and tested and have good agreement between measurements and simulations.**

***Index Terms*— Filter, laser micromachining, micromachining, 3-D printing, waveguide, *W*-band.**

I. Introduction

With frequencies rising to 100 GHz and beyond, the waveguide is becoming more and more popular, mainly due to its low loss characteristics. Conventionally, the waveguides are produced from metal through precisely controlled CNC milling or sometimes electroforming. Waveguide components fabricated by CNC milling with good measured performance have been demonstrated; examples can be found in *W*-band [1], [2], WR-4 band [3], and WR-3 band [4]. As the frequencies continue to increase, waveguide features are getting smaller and demanding tighter tolerances. CNC milling may fail to fulfill these demands due to its intrinsic limitations with regard to available cutter sizes, the wear or breakage of cutters, generation of defects and cracks due to mechanical stresses, and achievable aspect ratios. In addition, CNC machines are very expensive when tight tolerances are required.

Alternative manufacturing technologies have been actively explored to cope with the demand for high-dimensional accuracy and good surface quality for waveguide devices at millimeter-wave and submillimeter-wave frequencies. Among them, three techniques have been attracting the most attention and they are silicon deep reactive ion etching (DRIE) [5]–[8], LIGA-based thick resist electroplating [9], [10], and SU8 layered process [11]–[13]. Waveguides produced using these techniques are usually built from several silicon or polymer layers that are then metalized to achieve a good electrical conductivity. Then, the layers have to be assembled with high accuracy to form the waveguide devices. Such fabrication routes require multistep processing and clean room technologies. This makes the photoresist-based fabrication approaches relatively capital intensive and thus potentially viable only for relatively high batch sizes or for high added value components for application in niche markets. In addition, these methods have intrinsic limitations regarding the materials that can be processed and the type of structures that can be used in the design (e.g., only single height waveguide features are permitted in every layer).

Laser micromachining is another very attractive alternative fabrication technique. Compared with SU8- or silicon-based processes, laser micromachining offers some appealing advantages.

1) It allows all metal devices to be fabricated, and this is ideally suited to scenarios where a higher thermal stability of the devices is required.
2) It is capable of producing 3-D waveguide structures with varying depths (or heights) from one workpiece and thus eliminates the need for splitting the device into several layers and then assembling them with a high accuracy. This could yield an improved insertion loss and ultimately a better performance.
3) It is a direct write approach and small-to-medium-size batches of devices can be produced cost effectively while having a higher flexibility to introduce modification in the design. In comparison with CNC milling, laser micromachining can achieve smaller feature sizes with greater dimensional and geometrical accuracy. There is no tool wear or machine vibration due to cutting forces, as it is a noncontact process.

Manuscript received December 07, 2015; revised May 06, 2016; accepted May 25, 2016. Date of publication June 22, 2016; date of current version August 4, 2016. This work was supported by the U.K. Engineering and Physical Sciences Research Council (EPSRC) under Contract EP/M016269/1.

X. Shang and M. J. Lancaster are with the Department of Electronic, Electrical and Systems Engineering, University of Birmingham, Birmingham B15 2TT, U.K. (e-mail: x.shang@bham.ac.uk; m.j.lancaster@bham.ac.uk).

P. Penchev and S. Dimov are with the Department of Mechanical Engineering, University of Birmingham, Birmingham B15 2TT, U.K. (e-mail: PenchevP@adf.bham.ac.uk; s.s.dimov@bham.ac.uk).

C. Guo is with the Department of Electronic, Electrical and Systems Engineering, University of Birmingham, Birmingham B15 2TT, U.K., and also with the School of Physical Electronics, University of Electronic Science and Technology of China, Chengdu 610054, China (e-mail: spmguo@163.com).

Y. Dong is with the School of Physical Electronics, University of Electronic Science and Technology of China, Chengdu 610054, China (e-mail: dongyull@163.com).

M. Favre, M. Billod, and E. de Rijk are with Swissto12 SA, EPFL Innovation Park, Lausanne 1015, Switzerland (e-mail: m.favre@swissto12.ch; m.billod@swissto12.ch; e.derijk@swissto12.ch).

Color versions of one or more of the figures in this paper are available online at http://ieeexplore.ieee.org.

Digital Object Identifier 10.1109/TMTT.2016.2574839

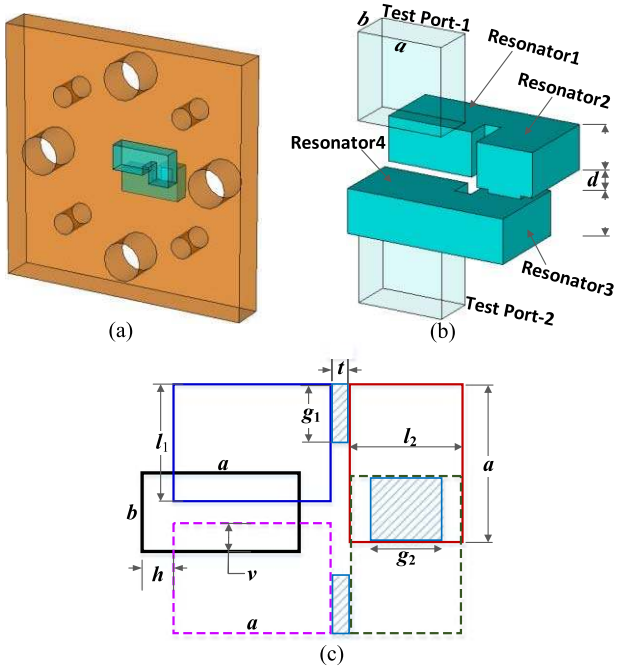

Fig. 1. Illustration of the *W*-band filter based on one single piece. This filter is for laser micromachining. (a) Overview of the filter including holes for UG-387 flange screws and pins. The turquoise blue surface represents the air volume inside the device. (b) Diagram of the filter structure with test input and output. Input/output waveguides are not parts of the filter. $a = 2.54$, $b = 1.27$, and $d = 0.1$. (c) Schematic top view diagram of the filter. The black rectangle represents the input/output waveguide of the test equipment. The blue hatched area stands for the coupling slots between resonators, and the resonators are represented using different colors. $l_1 = 1.941$, $l_2 = 1.683$, $g_1 = 1.252$, $g_2 = 0.995$, $t = 0.5$, $h = 0.5$, and $v = 0.536$ (mm).

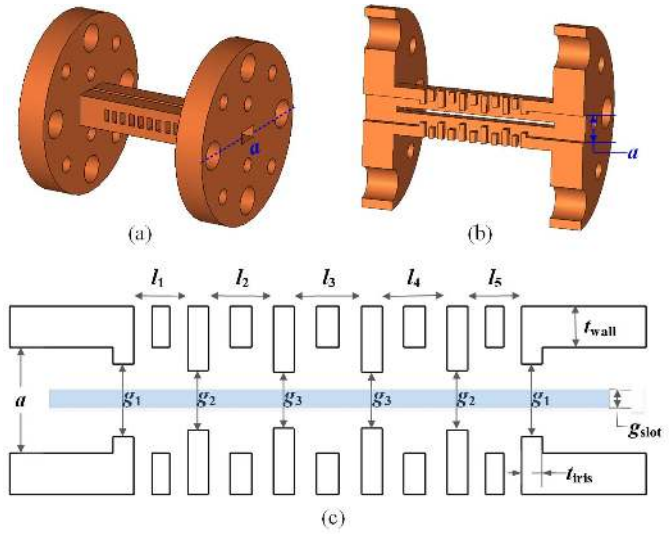

Fig. 2. Configurations of the fifth-order *W*-band filter with both broadside and narrow side slots. This filter is fabricated using 3-D printing. (a) Overview of the whole filter including two UG-387 flanges for microwave measurements. (b) Configuration of half of the filter, which is split along the dashed line shown in (a). (c) Schematic top view diagram of the filter (drawing not to scale). The blue rectangle stands for the slots on the middle of broadside wall. $a = 2.54$, $l_1 = l_5 = 1.311$, $l_2 = l_4 = 1.572$, $l_3 = 1.63$, $g_1 = 1.783$, $g_2 = 1.447$, $g_3 = 1.352$, $g_{\text{slot}} = 0.5$, $t_{\text{iris}} = 0.5$, and $t_{\text{wall}} = 1$ (mm).

In this paper, we introduce a laser-based micromachining technique for the fabrication of high-quality waveguide components incorporating features with varying depths. Laser micromachining is cost effective only when a relatively small volume of material has to be removed. Therefore, a hybrid manufacturing approach combining CNC milling with laser micromachining is proposed. More specifically, the conventional milling technology is employed to produce the mesoscale features such as assembly holes for alignment and fixing to a flange and thus to achieve a higher material removal rate. The functional filtering features of the waveguide devices are fabricated using laser micromachining to offer a relatively higher dimensional accuracy and good surface integrity. As a test of viability of the proposed technique, a fourth-order *W*-band filter, as shown in Fig. 1, is designed and fabricated using this hybrid process. This filter is designed to have a unique structure permitting double-side processing in a single setup, i.e., the entire filter structure can be made in one setup, without the need to mount/dismount the device several times. This yields a more accurate alignment and reduces setting up and machining time. Laser micromachining is reported to be utilized for the fabrication of various optical or quasi-optical components, such as metal mesh filters [14]. However, it is rarely utilized to produce submillimeter-wave waveguide components, except notably for a 2-THz horn antenna cut from silicon [15]. Here, for the first time, we present devices made from metal substrates directly. This eliminates the need for a metallization step and therefore yields a lower production cost with better durability of the devices.

Over the past two decades, there has been an increasing interest in the application of 3-D printing (also known as additive manufacturing) to manufacture components with high geometrical complexity. Some of the 3-D printing techniques have attracted a significant commercial interest and they are fused deposition modeling, stereolithography apparatus (SLA), and selective laser sintering (SLS) [16]. Among them, SLS is capable of printing all solid metal structures; however, such all metal components usually suffer from relatively poor electrical conductivities (high dissipative losses), considerable surface roughness, and dimensional inaccuracy [16]. SLA has found the most application in the production of passive waveguide components, as it offers the highest resolution and the best surface integrity [16]. In the open literature, 3-D printed antennas (see [17], [18]) and filters (see [18], [19]) are already reported. The merits of components made by 3-D printing are reduced fabrication time, reduced component weight (if made from plastics and plated with metal), elimination of the need for assembly, and increased design flexibility.

In this paper, a *W*-band waveguide filter (as shown in Fig. 2) is designed for an SLA-based 3-D printing technique with polymers. The filter is designed to have slots on both broadside and narrow side walls. This reduces the weight even further and facilitates the metal plating process allowing easy flowing of solution, while at the same time not having the penalty of degraded insertion loss. To date, most 3-D printed waveguide filters have been at frequencies well below 100 GHz, apart from a 107-GHz filter reported in [16]. The 3-D printing technology is improving with filters and components expected to increase in frequency. The filter presented here is centered

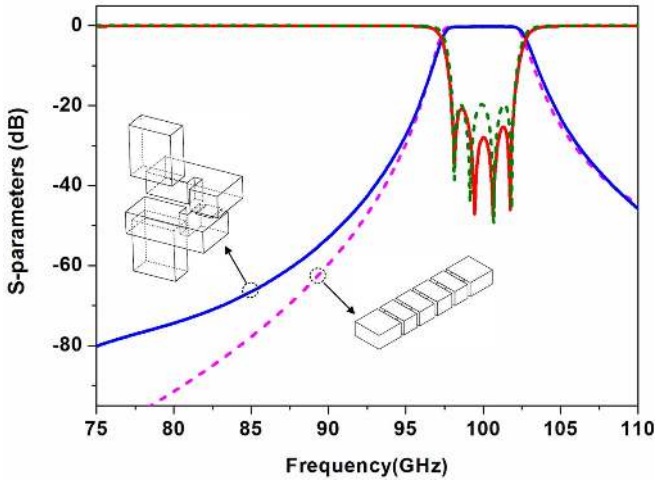

Fig. 3. Simulated S-parameters for the laser machined filter (solid lines) together with S-parameters of a conventional H-plane iris filter (dashed lines) with the same specifications.

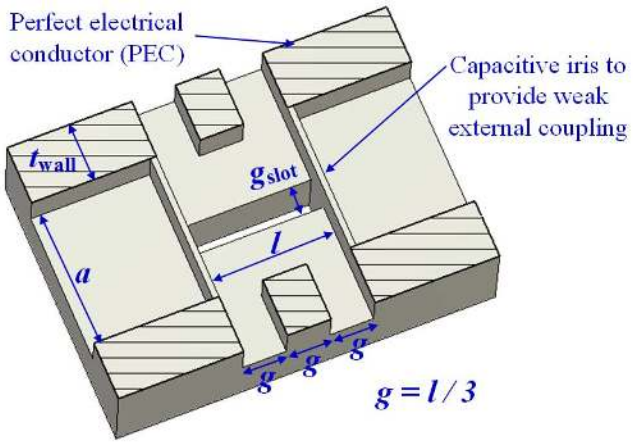

Fig. 4. Section view of a weakly coupled resonator with slots. $a = 2.54$, $l = 2.206$, $t_{\text{wall}} = 1$, and $g_{\text{slot}} = 0.5$ (mm).

at 90 GHz and represents one of the two highest frequency 3-D printed filters demonstrated to date.

Because this paper presents both laser micromachining and 3-D printed filters, it enables a comprehensive comparison of these two emerging technologies. This paper is organized as follows. Designs and structure details of the two filters are presented in Sections II and III, which is followed by a description of fabrication procedures in Section IV. Measurements and discussions are presented in Section V, and finally conclusions are given in Section VI.

II. Laser Machined Filter

The proposed filter for laser micromachining is shown in Fig. 1. It is based on four coupled resonators operating in the TE_{101} mode and has a Chebyshev response. The filter is designed by following a synthesis technique as described in [20] to have a center frequency of 100 GHz, an equal ripple bandwidth of 4%, and a passband return loss of 20 dB. To meet the filter specifications, the external Q and coupling coefficients between resonators are calculated to be [20] $Q_{e1} = Q_{e4} = 23.285$, $m_{12} = m_{34} = 0.0365$, and $m_{23} = 0.028$.

In order to be compatible with the laser micromachining process, the filter utilizes a special structure, as shown in Fig. 1(b). For this structure, the displacements between the feed waveguide and the first/fourth resonator control the external coupling (Q_e). The first and second resonators (or the third and fourth resonators) are coupled through an inductive iris and the coupling between resonators 2 and 3 is via a slot. Full-wave modeling for this filter is carried out using CST Microwave Studio (version 2015). Fig. 1(c) shows the detailed dimensions of this filter. The simulation results of the filter are shown in Fig. 3. The responses of a conventional H-plane iris coupled filter, with the same specification, is also included for comparison. As can be observed in Fig. 3, the out-of-band rejection of the laser machined filter is comparable to that of a conventional filter, but showing a slightly poorer rejection at the lower stopband. For the laser machined filter, both the input/output couplings and the coupling between resonators 2 and 3 are provided by structures that are equivalent to capacitive irises, and such irises are in fact resonant irises with their resonance frequency centered at the TE_{10} mode cut off of the feeding waveguide [21]. This is the reason for the poorer rejection at the lower stopband. In addition, the input/output coupling structures have a limitation on the filter's achievable bandwidth. It is difficult to obtain very low external quality factors, i.e., very large input/output coupling coefficients. According to CST simulations, the lowest external Q is calculated to be around 9 and this corresponds to a maximum fractional bandwidth of 10%. Despite the limitation on bandwidth and a relatively poor rejection at the lower stopband, in addition to the compatibility with laser machining, the filter offers the following advantages.

1) Lower insertion loss, as the first and last resonators are connected directly with the test ports (without the need to have connection waveguide at the two filter ends).
2) A standalone component eliminating any internal joints, which usually yields extra loss or requires precision assembling.
3) A reduction in size (more compact structure).

III. 3-D Printed Filter

The second filter, for 3-D printing, is a fifth-order Chebyshev filter with a center frequency of 90 GHz and an equal ripple bandwidth of 10 GHz. The passband return loss is designed to be 20 dB. Configurations of this filter are shown in Fig. 2.

As demonstrated in [22], two long slots, as wide as 9% of the waveguide internal width a, in the middle of broad side walls, do not contribute to any significant radiation loss to the filter. Here, the 3-D printed filter incorporates two such slots with a width of 0.5 mm. It also includes slots on the narrow side walls, as shown in Fig. 2(a) and (b). To understand the influence of slots on narrow side walls, a weakly coupled resonator, as shown in Fig. 4, is first considered. Simulations are performed in CST with a perfect electrical conductor;

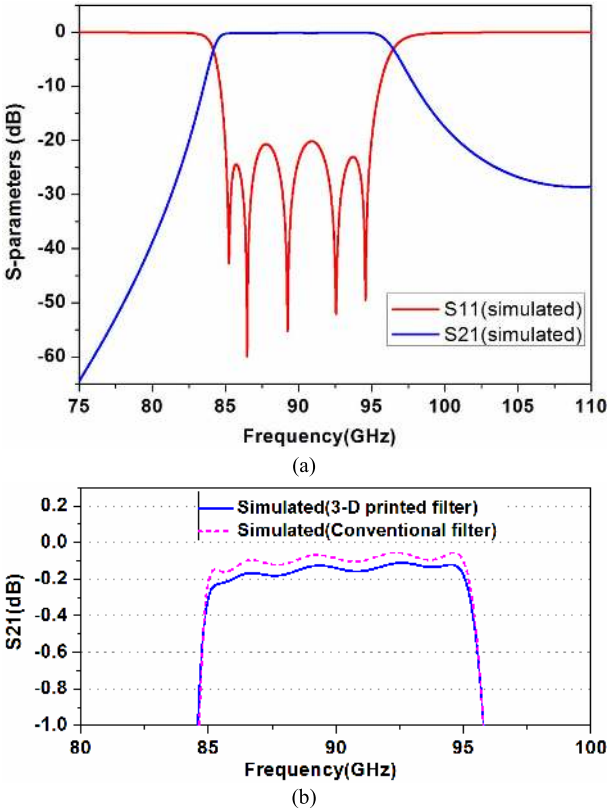

Fig. 5. (a) Simulated S-parameters for the 3-D printed filter. (b) Expanded view of S_{21} responses over the passband. The S_{21} responses of a conventional fifth-order H-plane iris filter (without slots) are also shown for comparison. All simulations are performed in CST using a conductivity of copper (5.96×10^7 S/m).

in other words, conductor loss is not taken into account. The quality factor of this resonator can be extracted from its simulated S_{21} response [20], and this indicates the amount of power radiated laterally out of the filter. Care must be taken to make the external couplings very weak so their influence on the radiation quality factor is negligible. As shown in Fig. 4, the resonator includes two slots at each side and each slot has a width of g (one third of resonator length) and a height of b. The radiation Q for the resonator with slots on narrow side walls is calculated to be around 99 000. After adding two slots on broadside walls, the radiation Q reduces to be around 52 000. This is still significantly larger than the quality factor associated with conductor loss, which is 2800 (calculated using a conductivity of copper and a resonant frequency of 90 GHz). It implies that slots on both the narrow side and broadside walls do not introduce any notable radiation. This is due to the fact in both cases, the current flowing paths are not cut by these slots.

From the filter's specifications, the external Q and nonzero coupling coefficients are calculated to be [20] $Q_{e1} = Q_{e5} = 8.7426$, $m_{12} = m_{45} = 0.0962$, and $m_{23} = m_{34} = 0.0707$. From these coupling coefficients, the dimensions of this filter can be extracted by following the procedure in [20]. The final dimensions are given in Fig. 2(c). Their corresponding simulated responses are shown in Fig. 5. This filter with slots exhibits an insertion loss very close to that of a conventional

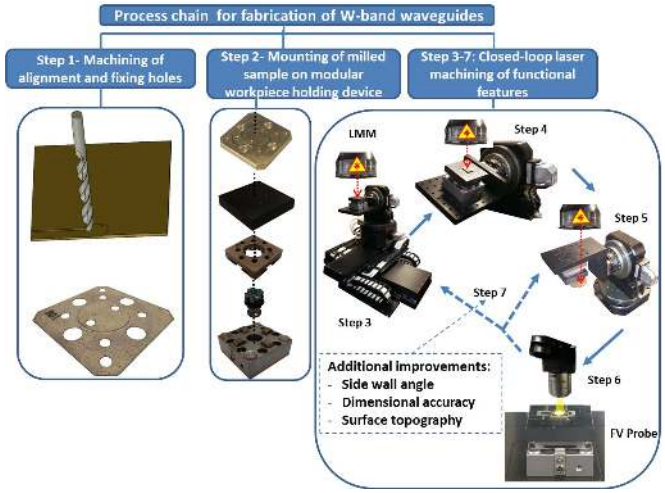

Fig. 6. Detailed design of the laser-based process chain for the fabrication of a laser machined filter.

inductive irises coupled filter with the same specifications but with no slots, as can be observed in Fig. 5(b). In addition, as shown in Fig. 5(a), the filter exhibits a relatively poor higher stopband (i.e., asymmetrical $|S_{21}|$ response), and this is attributed to the effect of resonances at higher harmonic frequencies and higher order modes.

IV. Fabrication Details

The laser machined filter is fabricated by utilizing a multistage processing chain (as shown in Fig. 6), which integrates conventional milling with laser micromachining and thus creates a novel manufacturing solution that exploits the specific advantages of both processes, i.e., the high removal rates of milling for machining of the alignment and fixing holes and the high machining resolution of laser processing for the fabrication of the small functional features. The implemented process chain includes: 1) a standard CNC milling machine and 2) laser micromachining platform that integrates an Yb-doped subpico 5-W laser sources (from Amplitude Systems). This operates at a central wavelength of 1030 nm and has a maximum repetition rate of 500 kHz. The system includes a 3-D scan head together with a stack of three linier and two rotary stages. It also includes a 100-mm telecentric focusing lens with a machining field view of 35 mm × 35 mm and with a beam spot diameter (at the focal plane) of 45 μm.

The fabrication steps of the laser machined filter can be summarized as follows.

1) Milling of the alignment and fixing holes on a brass plate.
2) Fixing of the brass plates on a modular workpiece holding device for the follow-up two-side laser machining of the waveguide functional structures.
3) Laser machining of one side of the filter structure.
4) Multiaxis machining employing the rotary stages to access sidewalls and produce vertical sidewalls (~90°).
5) Repositioning of the workpiece holding device at 180° employing one of the rotary stages and thus to gain access to the opposite side of the waveguide and then repetition of Steps 3) and 4).

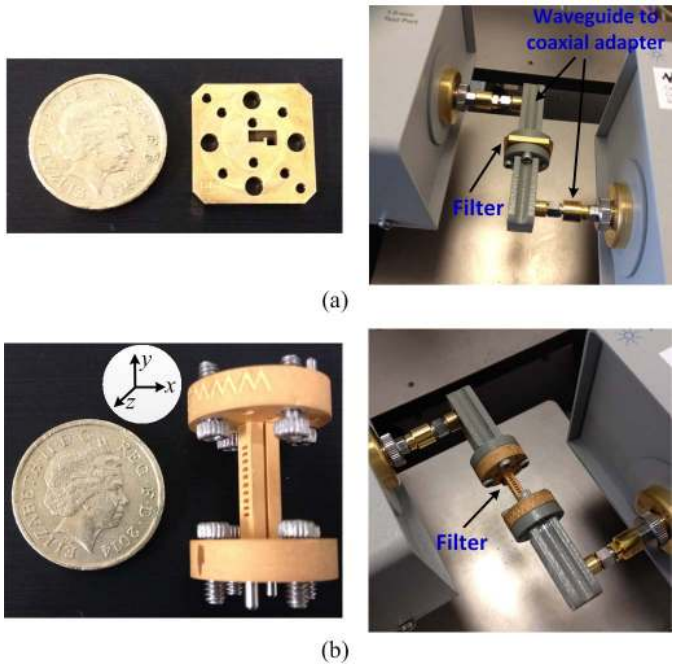

Fig. 7. (a) Photograph of the laser machined filter and the measurement setup. (b) Photograph of the 3-D printed filter and the measurement setup. Both filters are connected to two waveguides to coaxial adaptors, which are then connected to the test port of the network analyzer.

6) Inspection of the produced waveguide features using the Alicona InfiniteFocus microscope system to quantify their dimensional deviations from the nominal ones.
7) Final laser machining operations if there are any deviations from the nominal dimensions of the waveguide structures.

The utilized laser machining parameters are the average power of 4.2 W, pulse repetition frequency of 125 kHz, beam scanning speed of 0.5 m/s, and hatch pitch of 4 μm with a random hatching orientation. The total machining time is 90 min inclusive of the time required for alignment, repositioning, and inspection of the laser produced waveguide. Note that Step 5) involves rotations of stage and such machining operations have an evaluated accuracy, repeatability, and reproducibility better than 10 μm [23]. Furthermore, through careful optimization of the laser processing parameters, Step 7) could be eliminated from the process chain due to the very good repeatability of the laser micromachining operations. Further details of the process are given in [23].

It should be noted that the laser micromachining is capable of achieving a tolerance within 10 μm. This is for the machine used in the production of the filters and the tolerance is expected to improve considerably over time. This is a new technology and expectations are high. State-of-the-art CNC milling may achieve slightly tighter tolerance; however, it suffers from other problems such as very expensive milling machines to achieve it as well as breakage of cutters, availability of small cuter size, and generation of defects and cracks due to mechanical stresses. From this perspective, laser micromachining could be a promising alternative.

The 3-D printed filter is fabricated using a stereolithographic printing technique at Swissto12 [24]. The filter is printed out of nonconductive photosensitive resin layer by layer employing a UV laser and is subsequently coated with a 10-μm-thick copper all around. Then, the whole filter is passivated with a thin (around 100 nm) layer of gold to prevent it from oxidation. The final component has integrated self-aligning UG-387 flanges (including pins and screws) for quick and reliable connections, as shown in Fig. 7. More details about the fabrication process are provided in [24] and [25].

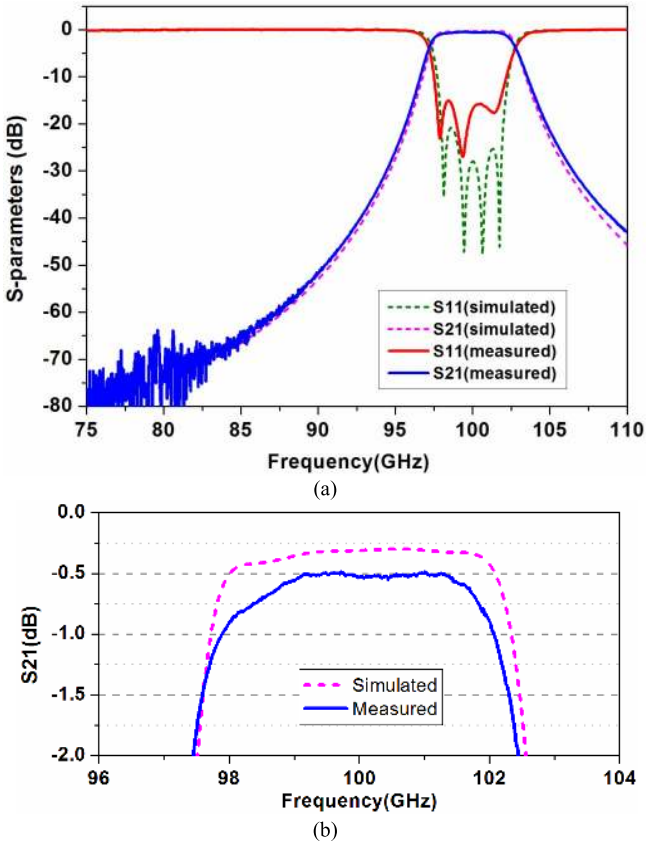

Fig. 8. Measurement results (solid lines) and simulation results (dashed lines) of the laser machined filter. (a) Responses over the whole W-band. (b) Expanded view of S_{21} over passband. The simulations are performed in CST using a conductivity of brass (2.74×10^7 S/m).

V. Measurement and Discussion

The S-parameter measurements of the two filters are performed on an Agilent E8361A network analyzer subject to a short–open–load–thru calibration. During the measurement, the laser machined filter is placed in the middle of two waveguide flanges of the network analyzer, as shown in Fig. 7(a). The four alignment pins of the waveguide flanges ensure the accuracy to which the brass filter is aligned to flanges of the network analyzer. The screws are utilized to achieve an intimate contact between the filter and flanges.

The S-parameter measurement results of the brass filter are shown in Fig. 8. There is excellent agreement between the measured performance and simulations. The passband insertion loss is measured to be around 0.65 dB, which is close to the expected value of 0.3 dB obtained from CST simulations

using the conductivity of brass (i.e., 2.74×10^7 S/m). The maximum passband return loss is measured to be 15 dB, whereas the simulated one is 20 dB. This difference provides around 0.1 dB of the loss in the S_{21} result. The rest, a 0.25-dB loss, is mainly be attributed to surface roughness of laser processed areas, which yields a reduced effective conductivity. The typical surface roughness values, measured with the Alicona InfiniteFocus microscope, are on the order of 1.25 μm. This reduces the effective conductivity to 7.04×10^6 S/m and results in an additional loss of 0.22 dB. The deviation in S_{11} responses is believed to be caused by small-dimensional inaccuracies (features on the top surface measured to be within 5 μm of nominal dimensions) and small misalignments during measurements. It should be noted that brass is selected here due to its good CNC machinability. This enables the precise production of alignment pin holes on the in-house CNC machine. To achieve a better performance in terms of insertion loss, the same design can be produced from copper workpieces using the proposed manufacturing platform. The only difference is the laser parameters, which will need to be adjusted slightly. In addition, surface roughness of laser processed areas can be reduced further by utilizing a top-hat beam shaper, which provides a more uniform energy distribution during the machining and thus a better surface roughness than that obtainable with a Gaussian laser beam (utilized in this paper).

The measurement setup for the 3-D printed filter is shown in Fig. 7(b). The filter is inserted in between two flanges, aligned using pins on the flange, and tightened using four screws. The measured responses of this 3-D printed filter are shown in Fig. 9. The measured central frequency of this filter shifts downward by around 2.5 GHz (2.78%). The measured averaged passband insertion loss is around 0.4 dB, whereas the simulated loss using a conductivity of copper is 0.15 dB. The measured return loss is better than 18 dB across the passband. The difference in insertion loss is small and may be attributed to a combination of factors including: 1) worse-than-simulated return loss (the worsening return loss contributes to an additional insertion loss of 0.026 dB) and 2) nonperfect surface quality (the surface roughness is measured to have a typical value of 1 μm. This degrades the effective conductivity to 1.52×10^7 S/m and yields an additional loss of around 0.13 dB).

The physical dimensions for the 3-D printed filter are measured using a microscope, and it is found that the measured dimensions in the x–y plane [see Fig. 7(b) for defined coordinate system] are approximately 4% larger than the designed and dimensions along the z-axis is roughly 1% larger than the designed. A modified model taking account of those fabrication inaccuracies is simulated in CST and the results are shown in Fig. 9. A very good agreement between the resimulation results and the measured responses is achieved. Compared with the originally designed structure, the modified model uses scaled dimensions with scale factors of 1.04, 1.04, and 1.01, for the x, y, and z directions, respectively.

It should be noted that the deviation in dimensions observed in this first proof-of-principle demonstrator filter is attributed

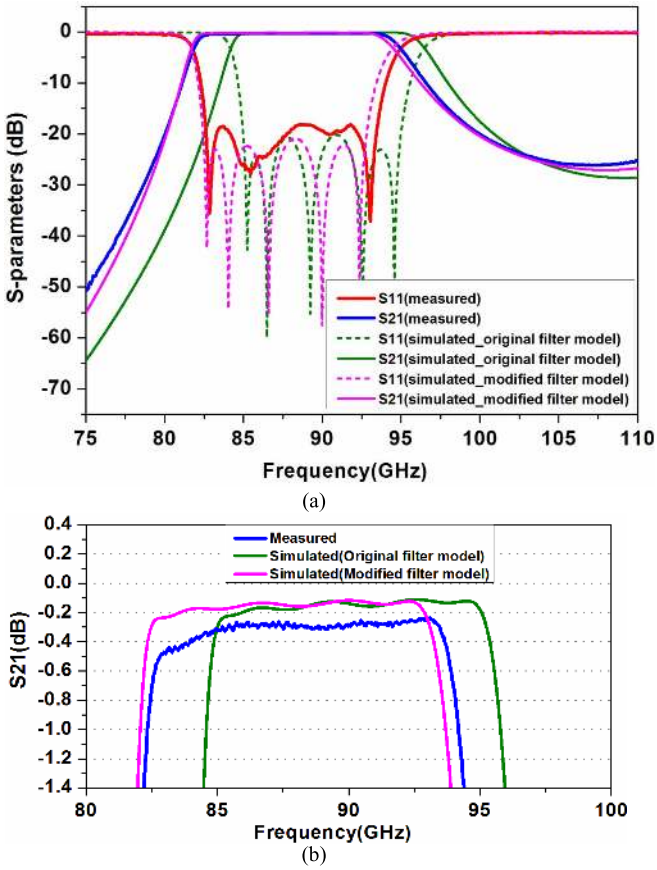

Fig. 9. Comparison of measurement and simulation results of the 3-D printed filter. (a) Responses over the whole *W*-band. Simulation results of both the original ideal filter model and the modified filter model with practical fabrication dimensions are shown. (b) Expanded view of S_{21} over passband.

to the postcuring step of the SLA printing process. It has been found out that such an enlargement (sometimes shrinkage) of dimensions is highly repeatable, and therefore, the model for printing could be adjusted accordingly to compensate during the second iteration.

Power handling is an important consideration with filters. The laser machined filter is made of brass, and thus it has an excellent thermal stability as well as a good power-handling capability. The 3-D printed filter is made out of resin-based polymer, which has a service temperature of from −65 °C to 85 °C. This may prevent the filter from being utilized in high-power applications. In this scenario, a material with a better thermal stability (e.g., ceramic-filled resin) can be used to print the same filter.

Table I shows the comparison of measurement performances of *W*-band waveguide filters realized using different types of manufacturing technique. All the filters summarized in Table I are based on coupled TE_{101} resonators and most filters use inductive irises for couplings, except for the one in [11] that uses capacitive irises and the laser machined filter described here, which utilizes both inductive and capacitive irises. In addition, a majority of the filters are constructed using split block technology, for which the filters are cut along the middle of the broadside wall for minimized loss. Table I indicates that the laser machined filter and 3-D printed filter

TABLE I
COMPARISON OF RECENTLY PUBLISHED *W*-BAND WAVEGUIDE BANDPASS FILTERS

f_0 (GHz)	Fractional bandwidth	Filter type	n	IL (dB)	RL (dB)	Manufacturing techniques	Reference
100	10%	Extracted pole filter with elliptical response	4	0.6	>18	CNC milling	[1]
92.6	4.53%	Chebyshev filter	4	0.5	>14	CNC milling	[2]
88.47	9.7%	Chebyshev filter	4	0.97~1.1	>15	SU-8 process	[11]
102	5%	Extracted pole filter with Pseudo-Elliptical response	4	1.2	>10	SU-8 process	[12]
107.2	6.34%	Chebyshev filter	6	0.95	>11	3-D printing	[16]
92.45	4.83%	Chebyshev filter	4	1.1~1.3	>10	DRIE	[26]
95	3.68%	Chebyshev filter	5	3.49	>18	Hot embossing	[27]
100	4%	Chebyshev filter	4	0.5~0.8	>15	Laser micromachining	This work
87.5	11.5%	Chebyshev filter	4	0.3~0.5	>18	3-D printing	This work

*f_0: center frequency of the filter; n: filter order; IL: passband insertion loss; RL: passband return loss.

demonstrate a comparable performance (in terms of low insertion loss and good return loss) to those made by high precision milling [1], [2].

VI. CONCLUSION

A laser-based micromachining platform and a stereolithography-based 3-D printing technique have been used to fabricate two *W*-band waveguide bandpass filters. These two filters have been specially designed to make the best use of the fabrication capability of each technique as well as the enabled flexibility in design. Both filters have been measured to have good performance. For the first time, laser micromachining, combined with CNC milling, has been utilized to produce millimeter-wave waveguide components from metal directly. The 3-D printed filter is also one of the just two waveguide filters demonstrated at millimeter-wave frequency band as high as *W*-band, using a 3-D printing technique.

This paper demonstrates the potential of employing laser-based micromachining and high-resolution stereolithography-based 3-D printing for small-to-medium-batch-size production of high-quality millimeter-wave and submillimeter-wave waveguide components.

REFERENCES

[1] C. A. Leal-Sevillano, J. R. Montejo-Garai, J. A. Ruiz-Cruz, and J. M. Rebollar, "Low-loss elliptical response filter at 100 GHz," *IEEE Microw. Wireless Compon. Lett.*, vol. 22, no. 9, pp. 459–461, Sep. 2012.

[2] X. Liao, L. Wan, Y. Yin, and Y. Zhang, "W-band low-loss bandpass filter using rectangular resonant cavities," *IET Microw., Antennas Propag.*, vol. 8, no. 15, pp. 1440–1444, Jul. 2014.

[3] C. A. Leal-Sevillano, T. J. Reck, G. Chattopadhyay, J. A. Ruiz-Cruz, J. R. Montejo-Garai, and J. M. Rebollar, "Development of a wideband compact orthomode transducer for the 180–270 GHz band," *IEEE Trans. THz Sci. Technol.*, vol. 4, no. 5, pp. 634–636, Sep. 2014.

[4] J.-X. Zhuang, W. Hong, and Z.-C. Hao, "Design and analysis of a terahertz bandpass filter," in *Proc. IEEE Int. Wireless Symp. (IWS)*, Shenzhen, China, Mar./Apr. 2015, pp. 1–4.

[5] Y. Li, B. Pan, C. Lugo, M. Tentzeris, and J. Papapolymerou, "Design and characterization of a *W*-band micromachined cavity filter including a novel integrated transition from CPW feeding lines," *IEEE Trans. Microw. Theory Techn.*, vol. 55, no. 12, pp. 2902–2910, Dec. 2007.

[6] X. H. Zhao *et al.*, "D-band micromachined silicon rectangular waveguide filter," *IEEE Microw. Wireless Compon. Lett.*, vol. 22, no. 5, pp. 230–232, May 2012.

[7] C. A. Leal-Sevillano *et al.*, "Silicon micromachined canonical E-plane and H-plane bandpass filters at the terahertz band," *IEEE Microw. Wireless Compon. Lett.*, vol. 23, no. 6, pp. 288–290, Jun. 2013.

[8] T. J. Reck, C. Jung-Kubiak, J. Gill, and G. Chattopadhyay, "Measurement of silicon micromachined waveguide components at 500–750 GHz," *IEEE Trans. THz Sci. Technol.*, vol. 4, no. 1, pp. 33–38, Jan. 2014.

[9] J. R. Stanec and N. S. Barker, "Fabrication and integration of micromachined submillimeter-wave circuits," *IEEE Microw. Wireless Compon. Lett.*, vol. 21, no. 8, pp. 409–411, Aug. 2011.

[10] E. D. Cullens, L. Ranzani, K. J. Vanhille, E. N. Grossman, N. Ehsan, and Z. Popovic, "Micro-fabricated 130–180 GHz frequency scanning waveguide arrays," *IEEE Trans. Antennas Propag.*, vol. 60, no. 8, pp. 3647–3653, Aug. 2012.

[11] X. Shang, M. Ke, Y. Wang, and M. J. Lancaster, "Micromachined W-band waveguide and filter with two embedded H-plane bends," *IET Microw., Antennas Propag.*, vol. 5, no. 3, pp. 334–339, Feb. 2011.

[12] C. A. Leal-Sevillano, J. R. Montejo-Garai, M. Ke, M. J. Lancaster, J. A. Ruiz-Cruz, and J. M. Rebollar, "A pseudo-elliptical response filter at W-band fabricated with thick SU-8 photo-resist technology," *IEEE Microw. Wireless Compon. Lett.*, vol. 22, no. 3, pp. 105–107, Mar. 2012.

[13] X. Shang, Y. Tian, M. J. Lancaster, and S. Singh, "A SU8 micromachined WR-1.5 band waveguide filter," *IEEE Microw. Wireless Compon. Lett.*, vol. 23, no. 6, pp. 300–302, Jun. 2013.

[14] B. Voisiat, A. Bičiūnas, I. Kašalynas, and G. Račiukaitis, "Band-pass filters for THz spectral range fabricated by laser ablation," *Appl. Phys. A*, vol. 104, no. 3, pp. 953–958, May 2011.

[15] C. K. Walker, G. Narayanan, H. Knoepfle, J. Capara, J. Glenn, and A. Hungerford, "Laser micromachining of silicon: A new technique for fabricating high quality terahertz waveguide components," in *Proc. 8th Int. Symp. Space THz Technol.*, Cambridge, MA, USA, Mar. 1997, pp. 358–376.

[16] M. D'Auria *et al.*, "3-D printed metal-pipe rectangular waveguides," *IEEE Trans. Compon., Packag., Manuf. Technol.*, vol. 5, no. 9, pp. 1339–1349, Sep. 2015.
[17] K. F. Brakora, J. Halloran, and K. Sarabandi, "Design of 3-D monolithic MMW antennas using ceramic stereolithography," *IEEE Trans. Antennas Propag.*, vol. 55, no. 3, pp. 790–797, Mar. 2007.
[18] B. Liu, X. Gong, and W. J. Chappell, "Applications of layer-by-layer polymer stereolithography for three-dimensional high-frequency components," *IEEE Trans. Microw. Theory Techn.*, vol. 52, no. 11, pp. 2567–2575, Nov. 2004.
[19] N. Delhote, D. Baillargeat, S. Verdeyme, C. Delage, and C. Chaput, "Ceramic layer-by-layer stereolithography for the manufacturing of 3-D millimeter-wave filters," *IEEE Trans. Microw. Theory Techn.*, vol. 55, no. 3, pp. 548–554, Mar. 2007.
[20] J.-S. Hong and M. J. Lancaster, *Microstrip Filters for RF/Microwave Applications*. New York, NY, USA: Wiley, 2001, pp. 257–271.
[21] G. F. Craven and R. F. Skedd, *Evanescent Mode Microwave Components*. Norwood, MA, USA: Artech House, 1987.
[22] X. Shang, M. J. Lancaster, and S. Dimov, "Microwave waveguide filter with broadside wall slots," *Electron. Lett.*, vol. 51, no. 5, pp. 401–403, Mar. 2015.
[23] P. Penchev, S. Dimov, D. Bhaduri, and S. L. Soo, "Generic integration tools for reconfigurable laser micromachining systems," *J. Manuf. Syst.*, vol. 38, pp. 27–45, Jan. 2016.
[24] Swissto12, Lausanne, Switzerland. (Nov. 2015). [Online]. Available: http://www.Swissto12.com
[25] A. Macor, E. de Rijk, S. Alberti, T. Goodman, and J.-P. Ansermet, "Three-dimensional stereolithography for millimeter wave and terahertz applications," *Rev. Sci. Instrum.*, vol. 83, no. 4, p. 046103, 2012.
[26] Y. Li, P. L. Kirby, and J. Papapolymerou, "Silicon micromachined W-band bandpass filter using DRIE technique," in *Proc. 36th Eur. Microw. Conf.*, Manchester, U.K., Sep. 2006, pp. 1271–1273.
[27] F. Sammoura, Y. Cai, C.-Y. Chi, T. Hirano, L. Lin, and J.-C. Chiao, "A micromachined W-band iris filter," in *Proc. 13th Int. Conf. Solid-State Sens., Actuators Microsyst.*, Jun. 2005, pp. 1067–1070.

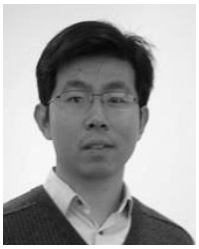

Xiaobang Shang (M'13) was born in Hubei, China, in 1986. He received the B.Eng. (Hons.) degree in electronic and communication engineering from the University of Birmingham, Birmingham, U.K., in 2008, the B.Eng. degree in electronics and information engineering from the Huazhong University of Science and Technology, Wuhan, China, in 2008, and the Ph.D. degree in microwave engineering from the University of Birmingham in 2011. His doctoral research concerned micromachined terahertz waveguide circuits and synthesis of multiband filters.

He has been a Research Fellow with the Department of Electronic, Electrical and Systems Engineering, University of Birmingham, since 2011. His current research interests include microwave filters and multiplexers, and MMIC amplifiers.

Pavel Penchev received the B.Eng. degree in mechanical engineering and the Ph.D. degree in laser microprocessing from the University of Birmingham, Birmingham, U.K., in 2012 and 2016, respectively.

He was a Research Associate with the Laser Micromachining Group, Advanced Manufacturing Technology Center, University of Birmingham, from 2013 to 2015, where he has been a Research Fellow since 2015. His current research interests include the implementation of reconfigurable laser platforms for addressing challenging technological requirements of complex multilength scale products and the generic system-level tools and techniques for improving the machine tool performance of reconfigurable laser processing platforms in relation to their process reliability, flexibility, and robustness.

Cheng Guo received the B.Eng. degree in communication engineering from Southwest Jiaotong University, Chengdu, China, in 2012. He is currently pursuing the Ph.D. degree at the University of Electronic Science and Technology of China, Chengdu, China.

His current research interests include 3-D printing of microwave devices and THz frequency multipliers/mixers.

Michael J. Lancaster (SM'04) was born in the U.K. in 1958. He received the B.Sc degree in physics and the Ph.D. degree in nonlinear underwater acoustics from Bath University, Bath, U.K., in 1980 and 1984, respectively.

He joined as a Research Fellow with the Surface Acoustic Wave Group, Department of Engineering Science, University of Oxford, Oxford, U.K., after leaving Bath University. In 1987, he became a Lecturer with the Department of Electronic and Electrical Engineering, University of Birmingham, Birmingham, U.K., lecturing in electromagnetic theory and microwave engineering. After he joined the Department of Electronic and Electrical Engineering, he began the study of the science and applications of high-temperature superconductors, in which he was involved in research on microwave frequencies. He was promoted to Head of the Emerging Device Technology Research Centre in 2000 and the Head of the Department of Electronic, Electrical and Computer Engineering in 2003. He has authored two books and over 190 papers in refereed journals. His current research interests include microwave filters and antennas, and the high-frequency properties and applications of a number of novel and diverse materials.

Prof. Lancaster is a Fellow of IET and the Institute of Physics in the U.K. He is a Chartered Engineer and Chartered Physicist. He has served on the IEEE MTT-S IMS Technical Committee.

Stefan Dimov received the Diploma Engineering and Ph.D. degrees from the Moscow State University of Technology, Moscow, Russia, in 1984 and 1989, respectively, and the D.Sc. degree from Cardiff University, Cardiff, U.K., in 2011.

He is currently a Professor of Micro Manufacturing and the Head of the Manufacturing Research Group with the School of Engineering, University of Birmingham, Birmingham, U.K. He has authored over 250 papers and co-authored two books. His current research interests include the wider areas of micro and advanced manufacturing technologies.

Prof. Dimov was a recipient of the Thomas Stephen Group Prize by the Institution of Mechanical Engineers in 2000 and 2003. He is an Associate Editor of the *ASME Journal of Micro- and Nano-Manufacturing* and the *Precision Engineering* journal. He initiated the European Network of Excellence in Multi-Material Micro Manufacture (4M), and is a Member of the Executive Boards of the 4M Association.

Yuliang Dong was born in Sichuan, China, in 1972. He received the B.S. degree in electronics engineering from Northwestern Polytechnical University, Xi'an, China, in 1993, and the Ph.D. degree from Beihang University, Beijing, China, in 2005.

He is currently an Associate Professor with the University of Electronic Science and Technology of China, Chengdu, China. His current research interests include microwave wave circuits, passive components, antennas, and microwave CAD technology.

Mirko Favre received the bachelor's degree in mechanical engineering from ETML, Lausanne, Switzerland, in 2001.

He held several successive mechanical engineering positions in research and development functions with the watchmaking industry (Swatch Group, Switzerland) and the medical technology industry (Xitact, Switzerland, and Toradex, Switzerland). He joined SWISSto12 SA, EPFL Innovation Park, Lausanne, in 2013, as a Project Manager and Mechanical Engineer, where he was involved in the development and production of additive manufactured RF waveguide, antenna, and filter products.

Mathieu Billod received the bachelor's degree in mechanical engineering from IUT Annecy, Annecy-le-Vieux, France, in 2007, and the master's degree in mechanical engineering from Polytech Annecy France, Annecy-le-Vieux, in 2011.

He held several successive mechanical engineering positions in research and development functions with the watchmaking industry (Swatch Group, Switzerland) and the semiconductor industry (Applied Materials, Switzerland). He joined SWISSto12 SA, EPFL Innovation Park, Lausanne, Switzerland, in 2013, as a Project Manager and Mechanical Engineer, where he was involved in the development and production of additive manufactured RF waveguide, antenna, and filter products.

Emile de Rijk received the bachelor's degree in physics from the Swiss Federal Institute of Technology in Lausanne (EPFL), Lausanne, Switzerland, in 2008, the master's degree in physics from the University of Amsterdam, Amsterdam, The Netherlands, and the Ph.D. degree in physics from EPFL in 2013.

He is currently a Co-Founder and CEO of SWISSto12, Lausanne, a company that spun-off from EPFL and pioneers the development and commercialization of radio-frequency antenna, waveguide, and filter products based on additive manufacturing.